applied sciences

MDPI

Article

Mineralogical Characterization of the Grot Lead and Zinc Mine Tailings from Aspects of Their Further Use as Raw Material

Jelena Gulicovski [1,*], Marija Stojmenović [1], Milena Rosić [1], Andrijana Vasić [1], Ivica Ristović [2], Ivona Janković-Častvan [3] and Milan Kragović [1]

[1] Institute of Nuclear Sciences, National Institute for the Republic of Serbia, University of Belgrade, Mike Petrovića Alasa 12-14, 11000 Belgrade, Serbia
[2] Faculty of Mining and Geology, University of Belgrade, Đušina 7, 11000 Belgrade, Serbia; ivica.ristovic@rgf.bg.ac.rs
[3] Faculty of Technology and Metallurgy, University of Belgrade, Karnegijeva 4, 11000 Belgrade, Serbia
* Correspondence: rocenj@vin.bg.ac.rs

Abstract: The possibility of using waste tailings produced by flotation in the lead and zinc mine of Grot, Serbia as a potential source of secondary mineral raw materials was examined. The aim of the research was primarily to carry out a detailed characterization in order to determine the dominant minerals, and, for the first time, to trace the changes occurring in the unit cells of the minerals present in that deposit. There was also a need to determine the exact proportions of the present mineral phases for their further application and utilization as natural resources in environmental protection. Samples were taken from three different sections of tailings: the crest of dam (JKB), outlet pipe of the flotation facility (JOF) and hydrocyclone overflow (JHC). Granulometric separation was performed to facilitate the extraction of certain minerals from waste. The results showed that all samples mainly contained quartz, clinochlore, calcite, albite, pyrite and biotite, but their ratios in each sample varied significantly. After characterization, samples were separated into different fractions and their mineralogical compositions were determined. Depending on the fraction, the mineralogical compositions also changed. Mineralogy and geochemical analysis indicate that waste tailings can be used as a secondary mineral raw materials source applicable in various industries.

Keywords: tailings; minerals extraction; mineralogy; geochemical properties; granulometry; byproduct valorization

check for updates

Citation: Gulicovski, J.; Stojmenović, M.; Rosić, M.; Vasić, A.; Ristović, I.; Janković-Častvan, I.; Kragović, M. Mineralogical Characterization of the Grot Lead and Zinc Mine Tailings from Aspects of Their Further Use as Raw Material. *Appl. Sci.* **2024**, *14*, 1167. https://doi.org/10.3390/app14031167

Academic Editors: Nikolaos Koukouzas and Fernando Rocha

Received: 18 December 2023
Revised: 23 January 2024
Accepted: 24 January 2024
Published: 30 January 2024

Copyright: © 2024 by the authors. Licensee MDPI, Basel, Switzerland. This article is an open access article distributed under the terms and conditions of the Creative Commons Attribution (CC BY) license (https://creativecommons.org/licenses/by/4.0/).

1. Introduction

Industrial development has contributed to the growth of the global economy, but on the other side, it has led to environmental degradation. In developed countries, problems related to environmental degradation have been mainly solved by introducing new technologies and strict regulations. However, due to the increased demand for natural resources, their exploitation is still active and related environmental problems are present. In contrast to developed countries, in developing countries, more environmental problems exist whose resolution has not even begun, and which are mainly related to unresolved historical pollution or the generation of waste polluted by different hazardous chemicals and materials. Mining is always followed by the production of waste which is deposited in nature in the form of tailings. The waste materials are often very noticeable, located near water resources, underinsured, or in areas with tourist or agricultural potential.

Mining is one of the most significant industries in Serbia. Of the total gross domestic production in the Republic of Serbia, metallurgy accounts for 10% of the total manufacture of basic metals and metal products [1]. The Grot Mine is one of the biggest and most significant, located in southeastern Serbia and mainly exploiting lead and zinc ores. The total content of lead and zinc in the ore is about 10.5 wt %, which indicates that about 90 wt % is waste material. The flotation process has generated around 5.5 million tons of waste

material until now, mostly in a state of biological vacuum [2]. The area around the Grot Mine is mostly composed of crystalline shales, predominantly of the Early Paleozoic and, to a lesser extent, of the Proterozoic age, with larger and smaller masses of Paleozoic and Triassic granitoid rocks and large Surdulic Paleogene granodiorite plutons. The Grot Mine represents a geo-economic unit within the Paleozoic metamorphic shale complex of the Serbian–Macedonian mass, located on the eastern perimeter of the Surdulian granodiorite. The minefield is located in a crystalline nucleus, located between the Carpatho-Balkanids in the east and the Vardar zone in the west [3]. In the Metallogenic Region of Besna Kobila, the ore deposits are related to Neogene volcanic–plutonic complexes. Mineral associations consist of sulfides of lead and zinc, locally copper and/or molybdenum. In the morpho-structural sense, the deposits are of the quadruple/impregnation type, hydrothermal-wire, lens-plate, metasomatic and wire-impregnation types [4]. The deposits were formed by metasomatic alteration of marble and calcschist under the influence of hydrothermal solutions rich in Pb, Zn and Cu. Vertical mineralization intervals are over 400 m [5]. Based on hydrogeological features, this granodiorite massif is characterized by a large area of open cracks and medium water permeability [6].

The landscape surrounding the Grot tailings is mostly mountainous. Environmental protection in the area that surrounds the locality where tailings are placed represents a significant problem. A possible solution may be given based on determining the geochemical properties of the waste materials and finding their potential application. Namely, although it is well known that this kind of waste poses a negative influence on the environment [7], it can contain a significant number of different valuable elements and minerals [8]. Thus, reprocessing of tailings reduces dependence on reserve extraction [9] and can provide economic and environmental benefits, which is completely in agreement with the circular economy and the Sustainable Development Goals [10,11]. In general, the area of the Western Balkans is rich in lead, zinc and copper ores, which is why there are a large number of mines in this area, both abandoned and active, and consequently leading to the generation of millions of tons of waste. Bearing in mind that the mines are from the same geological area, they have a very similar chemical and geological composition, and the detailed content of important chemical elements in the tailings of important mines in the Western Balkans is given in the work of Shain et al. [11].

This research is a continuation of previous research [12], which was related to the preliminary characterization of the crest of the dam (JKB), outlet pipe of the flotation facility (JOF) and hydro-cyclone overflow (JHC). In the presented paper, the accent is on the detailed mineralogical characterization of the JKB, JOF and JHC, in order to find a useful value for dominant minerals extracted from tailings and, at the same time, find potential solutions for lowering the total amount of waste materials in tailings to meet the criteria of zero waste and preserve the environment.

2. Materials and Methods

A sampling of the JKB, JOF and JHC was performed based on observations of the diversity of deposited material based on grain size, the colour of deposited material, different mechanical properties and the spatial distribution of material on the flotation tailings. A total of 10 probes were collected from the entire tailings: three probes were taken from the crest of the dam (JKB), two probes were conducted on the perimeter of the dam (JHC) and five probes were taken from the tailings plateau (JOF), Figure 1. All samples were dried in an oven at 105 °C. For every sample, probes were mixed and homogenized, and one representative sample (marked as JKB, JOF and JHC) was made and used for investigations.

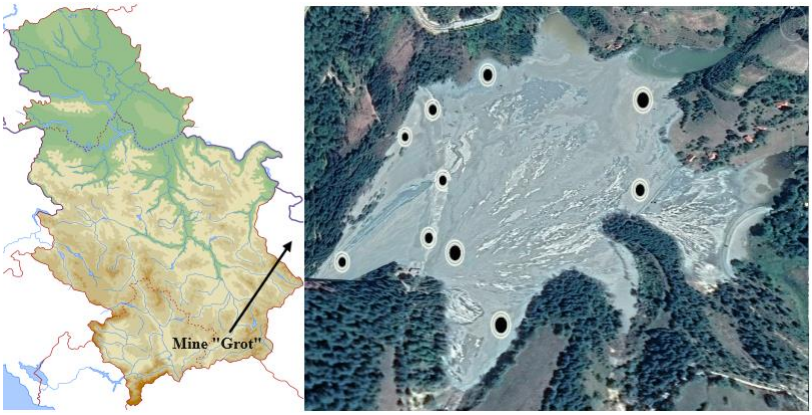

Figure 1. Sampling locations.

XRD was performed by using an Ultima IV Rigaku diffractometer (XRPD, Rigaku Ultima IV, Tokyo, Japan), equipped with CuK$\alpha_{1,2}$ radiations, using a generator voltage of 40.0 kV and a generator current of 40.0 mA. The range of 5–90° 2θ was used for all powders in a continuous scan mode with a scanning step size of 0.02° and at a scan rate of 10°/min, using a D/TeX Ultra-high-speed detector. a glass sample carrier was used for sample preparation. The unit cell parameters, volume of the unit cell and fractions of the phases were calculated by using the software package Powder Cell [13,14]. All the structural models for refinement, i.e., cif files of quartz, clinochlore, albite, biotite, pyrite and calcite were taken from the ICSD database [15].

The chemical compositions of the samples were determined by the classical chemical analysis of the aluminosilicates [16]. The concentrations of heavy metals were determined using a Perkin Elmer Analyst 300 (Perkin Elmer, Waltham, MA, USA) instrument for atomic absorption spectrometry (AAS).

Thermogravimetric (TGA), differential thermal analysis (DTA) and differential thermogravimetric analysis (DTG) of samples were performed on a Netzsch STA 409 EP (Netzsch, Selb, Germany). Samples were heated from 25 °C to 1000 °C in an air atmosphere at the heating rate of 10 °C/min. Before analysis, samples were kept in a desiccator at a relative humidity of 23%.

The morphology and microstructure of all samples were studied by field emission scanning electron microscopy (FESEM) with a TESCAN Mira3 XMU (Tescan, Kohoutovice, Czech Republic) at 20 kV. The samples were precoated with a 2–3-nanometre-thick layer of gold before observation. The images were recorded at a magnification of 10,000× with an accelerating voltage of 20 kV.

In order to determine which mineral is dominant in which fraction, JKB, JOF and JHC samples were sifted through different sieves. Fractions of tailings were separated with the following particle size: −63 + 0 μm, −100 + 63 μm, −200 + 100 μm, −300 + 200 μm, −400 + 300 μm and +400 μm, and all fractions were analyzed by the XRD method.

3. Results and Discussion

3.1. XRD Analysis of Tailings Samples

Structural characteristics of the JKB, JOF and JHC samples were investigated by using XRD, and the obtained results are presented in Figure 2 and Table 1. As observed in Figure 2a, all three analyzed samples exhibit a well-defined crystalline and a distinct mineralogical composition. Notably, the samples contain the following minerals: quartz, clinochlore, albite, biotite, pyrite and calcite [17–23]. From Figure 2b and Table 1, it is indisputable that the JKB and JOF samples possessed very similar compositions, and the most abundant minerals were quartz (~21–25%), clinochlore (~20–27%), albite (~28–31%) and calcite (~13–14%), while the presence of other minerals was in lower amounts (pyrite

(~1–5%); biotite (~6–8%)). A detailed description of the unit cell parameters of the minerals present is given in the Supplementary Material in the form of Table S1.

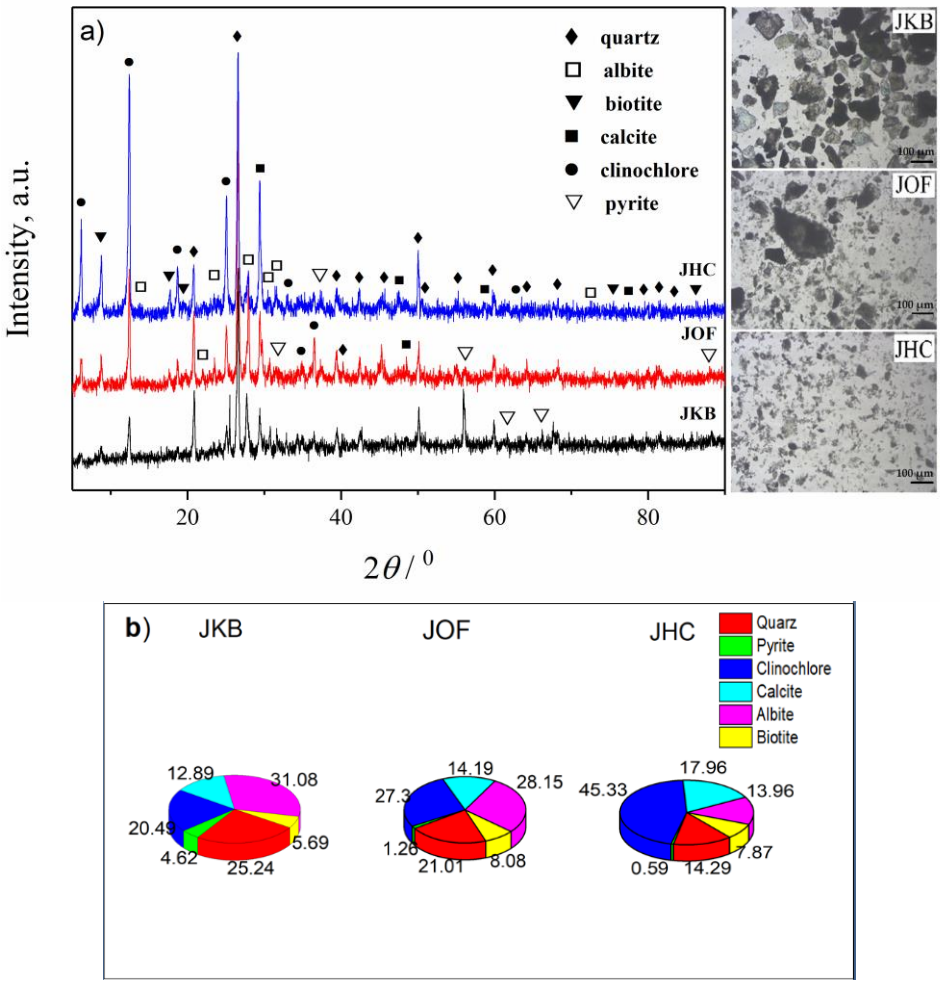

Figure 2. (**a**) XRD patterns and microphotography of examined samples; inset samples images obtained by optical microscopy; (**b**) Estimated mass percentages for the mineral composition of examined samples.

Table 1. The percentages of individual crystal phases (f/%), obtained using the software package Powder Cell, for examined samples.

Phase	JKB	JOF	JPH
Quartz; SiO_2	$f = 25.24$	$f = 21.01$	$f = 14.29$
Pyrite; FeS_2	$f = 4.62$	$f = 1.26$	$f = 0.59$
Clinochlore; $Mg_{2.5}Fe_{1.65}Al_{1.5}Si_{2.2}Al_{1.8}O_{10}(OH)_8$	$f = 20.49$	$f = 27.30$	$f = 45.33$
Calcite; $CaCO_3$	$f = 12.89$	$f = 14.19$	$f = 17.96$
Albite; Na ($Al\ Si_3\ O_8$)	$f = 31.08$	$f = 28.15$	$f = 13.96$
Biotite $K_2(Mg_{3.15}Fe_{2.59}Ti_{0.17}Mn_{0.09})\ (Si_{5.98}Al_{1.92}Ti_{0.10})O_{20}\ ((OH)_{1.47}F_{1.98})$	$f = 5.69$	$f = 8.08$	$f = 7.87$

In the crystal phase of the JHC sample, clinochlore was largely present (~45%), while the contents of other minerals were: ~18% calcite, ~14% albite and quartz, ~8% biotite and ~1% pyrite. Although not all Miller indices were visible in the diffractograms due to overlapping reflections, good crystallinity was evident in all samples. Micrographs presented in the inset of Figure 2 showed that particle size was the highest for JKB sample,

and lowest for the JHC sample. Results give information that in the waste materials taken from different parts of tailings are present minerals which possess properties for practical application, such as albite (in manufacturing of glass or ceramic) [19,20], calcite (in lime production and the construction industry) [21] and biotite (a filler and extender in paints, an additive to drilling muds, an inert filler and mold-release agent in rubber products) [22,23], and thus, waste material taken from the tailings may be used as a source for their extraction. In this way, by applying appropriate technologies, the extraction of useful minerals from the tailings may lead to the reduction of waste in nature and its environmental impact, while at the same time, natural resources would be fully utilized.

3.2. Chemical Composition

The results obtained by classical chemical analysis of the tailings samples taken from different places—JKB, JOF and JHC—are given in Table 2.

Table 2. Chemical composition of the tailings of the flotation facility of the Grot Mine [12].

Chemical Content	Content, %		
	JKB	JOF	JHC
SiO_2	40.09	53.62	48.61
Al_2O_3	8.68	10.52	12.94
CaO	9.08	8.73	9.33
MgO	1.86	2.15	2.74
Fe_2O_3	16.46	10.42	11.8
Na_2O	0.75	0.97	0.98
K_2O	1.46	1.94	2.10
TiO_2	1.01	0.84	1.01
Mn	1.05	1.17	1.14
S	8.07	2.14	1.52
Loss on ignition	10.67	6.91	7.23

The contents of Mg, K and Na, as well as Mn and Ti, were much lower, and these elements were mainly present in the form of clinochlore, albite and biotite. According to the results of chemical analyses, a significant difference between the three investigated samples was in the content of Fe (11.5%, 7.3 % and 8.3% for JKB, JOF and JHC, respectively) which was present in the form of pyrite, clinochlore and biotite, and in the content of sulfur. The content of sulfur in JKB (~8.07%; Table 1) was about four times higher in comparison with that of JOF and JHC (~2) [16]. Higher amounts of Fe and S obtained for JKB may be explained by a higher content of pyrite in comparison with JOF and JHC. Also, the contents of sulfur and pyrite in the investigated samples were not stochiometric, meaning that sulfur was also present in the samples in some other form. The results presented in Table 2 also show that, in all samples, there is a significant loss of mass by ignition, which mainly originates from organic additives, which are added during the ore processing, whose composition includes sulfur, which may be an explanation for the presence of sulfur which has not derived from pyrite.

3.3. Thermal Analyses (DTA/TGA/DTG)

Thermal analyses were used to confirm the presence of some of the most important mineral components in the JKB, JHC and JOF samples and results are given in Figure S1.

For all samples, it is evident that in the first temperature interval (25–400 °C), due to low humidity, significant peaks at DTA curves, as well as weight losses recorded by TGA, were not recorded. The indication that dehydration and releasing of loosely bound surface water occurs is visible across peaks at 117, 132 and 103 °C at DTG curves for JKB, JOF and JHC, respectively. The exothermic peaks at DTA curves at 478 °C for JOF and JHC and 493 and 535 °C for JOF and JKB were obtained in the second temperature interval (400–650 °C). In the same temperature range, peaks are visible at DTG curves as follows: 477 and 520 °C

for JKB, 573 °C for JOF and 551 °C for JHC, and adequate weight losses are visible at TGA curves. The shape of the thermal diagrams has been explained in the literature in various ways. According to [24], the peak at 478 °C for JOF and JHC and 493 °C for JKB can be explained by the presence of pyrite in the samples and its endothermic decomposition to Fe_2O_3 and SO_3, which can be estimated as follows:

$$4FeS_2 + 15O_2 \rightarrow 2Fe_2O_3 + 8SO_3 \quad (1)$$

The presence of a peak at 535 °C can be explained by additional decomposition of the Fe_2O_3, which explains why it was not detected by XRD analysis [25]. According to Steudel et al. [26], the DTA and DTG peaks in the second temperature range are indications of the presence of the clinochlore and are the result of its thermal degradation. Endothermic peaks with minima at 796, 812 and 775 °C were visible for all samples in the third temperature range (650–1000 °C) at DTA curves, i.e., at 787, 806 and 760 °C at DTG curves for JOF, JKB and JHC, respectively. These peaks are characteristic of the thermal decomposition of carbonates and originated from calcite ($CaCO_3$) which was also detected by XRD analyses. Due to the release of CO_2, the decomposition of calcite was followed by weight loss of 5.66, 6.41 and 6.03% for JOF, JKB and JHC, respectively.

3.4. Morphological Properties (FESEM Analysis and Optical Microscopy)

Micrographs of samples observed by FESEM and optical microscopy are given in Figure 3. In the presented micrographs, grains with corroded edges, in different shapes and dimensions, were observed in Figure 3. Corrosion originates from the chemicals which were used in ore flotation. The particle sizes ranged from 30 × 80 µm up to 150 × 300 µm, which was also confirmed by granulometry. SEM images of all the samples showed easily noticeable particles with bigger dimensions corresponding to the sulfide and carbonate classes of minerals, while the smaller ones, in the form of glued particles, correspond to the silicate class of minerals.

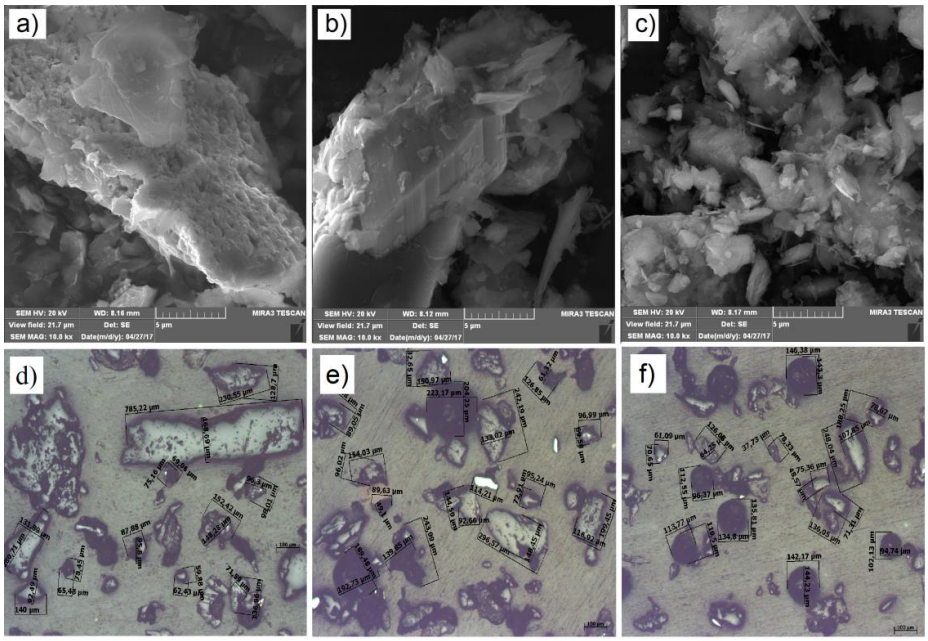

Figure 3. SEM images of the: (**a**) JKB, (**b**) JOF, (**c**) JHC, (**d**) JKB, (**e**) JOF and (**f**) JHC; (**d**–**f**) with the particle size obtained by optical microscopy.

3.5. Analysis of Tailings Fractions

After analyses, starting samples were sifted through different sieves and separated into particles ranging in different sizes. The percentages of individual fractions are given in Table 3.

Table 3. Contribution of individual fractions for JKB, JHC and JOF samples.

	JKB	JHC	JOF
Particle size, μm		Contribution, %	
+400	-	-	2.99
−400 + 300	1.36	-	5.02
−300 + 200	3.21	-	10.46
−200 + 100	40.89	0.54	31.61
−100 + 63	37.91	8.13	16.66
−63 + 0	16.73	91.33	33.27

The purpose was to investigate whether it is possible to concentrate or extract the individual crystalline phases, or to examine, whether and in which way, the crystalline phases present in the tailings are arranged concerning the particle size. All fractions were analyzed by the XRD method and the results are shown in Figures 4–7 and Tables 4–7 and S2–S5.

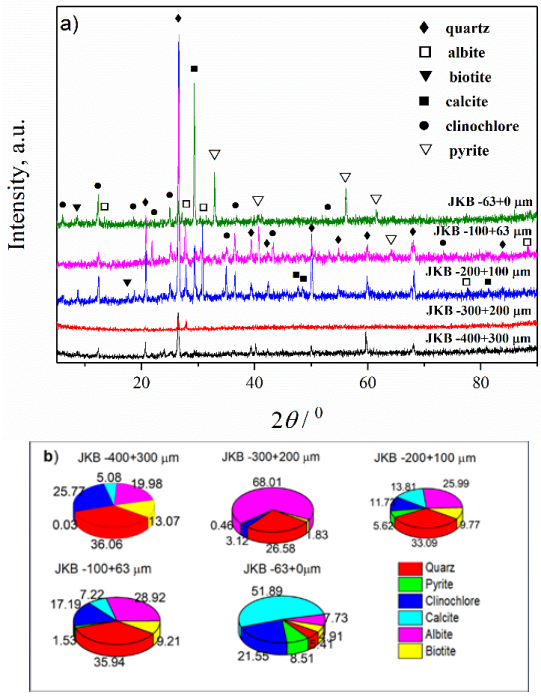

Figure 4. (**a**) XRD patterns of the JKB sample; (**b**) Estimated mass percentages for the mineral composition of the JKB sample.

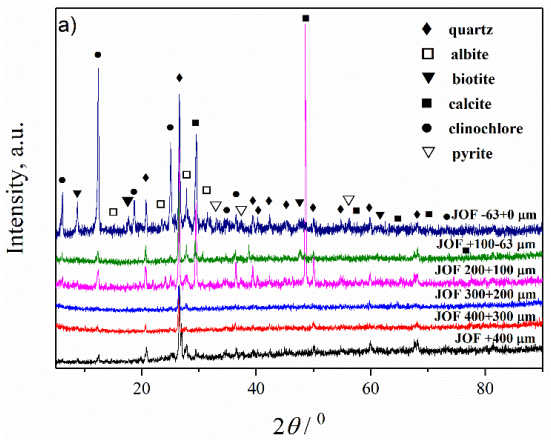

Figure 5. *Cont.*

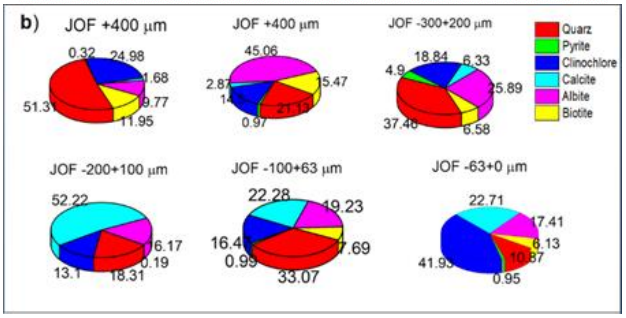

Figure 5. (**a**) XRD patterns of the JOF sample; (**b**) Estimated mass percentages for the mineral composition of the JOF sample.

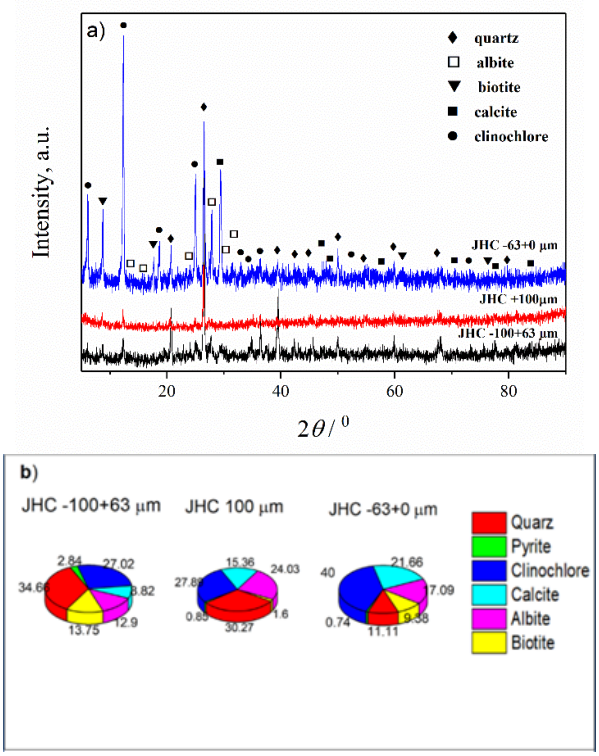

Figure 6. (**a**) XRD patterns of the JHC sample; (**b**) Estimated mass percentages for the mineral composition of the JHC sample.

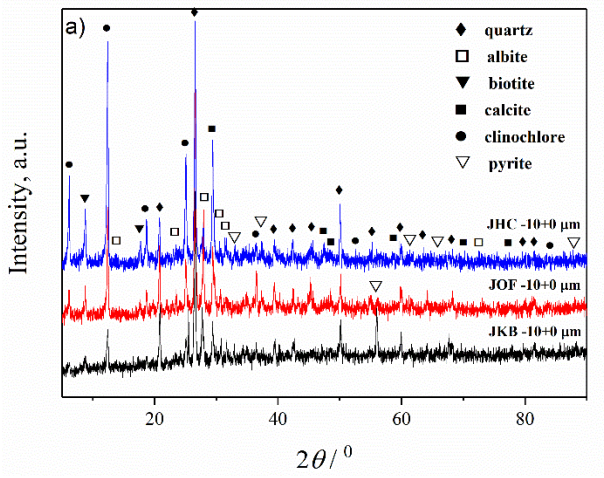

Figure 7. *Cont.*

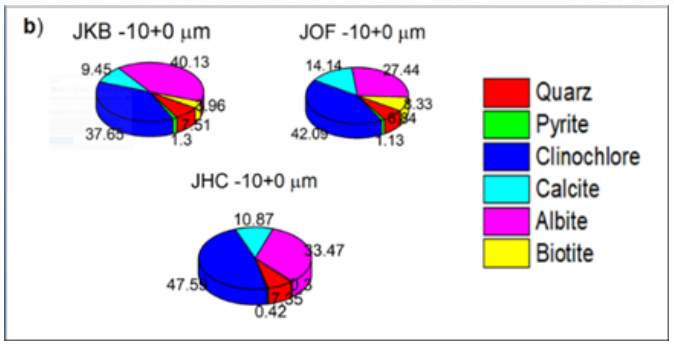

Figure 7. (**a**) XRD patterns of JKB, JOF and JHC samples of fraction −10 + 0 μm; (**b**) Estimated mass percentages for the mineral composition of JKB, JOF and JHC samples.

Table 4. The percentages of individual crystal phases (*f*/%), obtained using the software package Powder Cell, of different fractions for the JKB sample.

Phase	−400 + 300 μm	300 + 200 μm	200 + 100 μm	−100–63 μm	−63 + 0 μm
Quartz; SiO_2	*f* = 36.06	*f* = 26.58	*f* = 33.09	*f* = 35.94	*f* = 5.41
Pyrite; FeS_2	*f* = 0.03	/	*f* = 5.62	*f* = 1.53	*f* = 8.51
Clinochlore; $Mg_{2.5}Fe_{1.65}Al_{1.5}Si_{2.2}Al_{1.8}O_{10}(OH)_8$	*f* = 25.77	*f* = 3.12	*f* = 11.73	*f* = 17.19	*f* = 21.55
Calcite; $CaCO_3$	*f* = 5.08	*f* = 0.46	*f* = 13.81	*f* = 7.22	*f* = 51.89
Albite; Na ($AlSi_3O_8$)	*f* = 19.98	*f* = 68.01	*f* = 25.99	*f* = 28.92	*f* = 7.73
Biotite; $K_2(Mg_{3.15}Fe_{2.59}\ Ti_{0.17}Mn_{0.09})\ (Si_{5.98}Al_{1.92}Ti_{0.10})O_{20}\ ((OH)_{1.47}F_{1.98})$	*f* = 13.07	*f* = 1.83	*f* = 9.77	*f* = 9.21	*f* = 4.91

Table 5. The percentages of individual crystal phases (*f*/%), obtained using the software package Powder Cell, of different fractions for the JOF sample.

Phase	+400 μm	400 + 300 μm	300 + 200 μm	200 + 100 μm	−100–63 μm	−63 + 0 μm
Quarz; SiO_2	*f* = 21.13	*f* = 51.31	*f* = 37.46	*f* = 18.31	*f* = 33.07	*f* = 10.87
Pyrite; FeS_2	*f* = 0.97	*f* = 0.32	*f* = 4.90	/	*f* = 0.99	*f* = 0.95
Clinochlore; $Mg_{2.5}Fe_{1.65}Al_{1.5}Si_{2.2}Al_{1.8}O_{10}(OH)_8$	*f* = 14.50	*f* = 24.98	*f* = 18.84	*f* = 13.10	*f* = 16.74	*f* = 41.93
Calcite; $CaCO_3$	*f* = 2.87	*f* = 1.68	*f* = 6.33	*f* = 52.22	*f* = 22.28	*f* = 22.71
Albite; Na ($AlSi_3O_8$)	*f* = 45.06	*f* = 9.77	*f* = 25.89	*f* = 16.17	*f* = 19.23	*f* = 17.41
Biotite; $K_2(Mg_{3.15}Fe_{2.59}Ti_{0.17}Mn_{0.09})\ (Si_{5.98}Al_{1.92}Ti_{0.10})O_{20}((OH)_{1.47}F_{1.98})$	*f* = 15.47	*f* = 11.95	*f* = 6.58	*f* = 0.19	*f* = 7.69	*f* = 6.13

Table 6. The percentages of individual crystal phases (*f*/%), obtained using the software package Powder Cell, of different fractions for the JHC sample.

Phase	−100 + 63 μm	−200 + 100 μm	−63 + 0 μm
Quarz; SiO_2	*f* = 34.66	*f* = 30.27	*f* = 11.11
Pyrite; FeS_2	*f* = 2.84	*f* = 0.85	*f* = 0.74
Clinochlore; $Mg_{2.5}Fe_{1.65}Al_{1.5}Si_{2.2}Al_{1.8}O_{10}(OH)_8$	*f* = 27.02	*f* = 27.89	*f* = 40.00
Calcite; $CaCO_3$	*f* = 8.82	*f* = 15.36	*f* = 21.66
Albite; Na ($Al\ Si_3\ O_8$)	*f* = 12.90	*f* = 24.03	*f* = 17.09
Biotite; $K_2(Mg_{3.15}Fe_{2.59}\ Ti_{0.17}Mn_{0.09})\ (Si_{5.98}Al_{1.92}Ti_{0.10})O_{20}\ ((OH)_{1.47}F_{1.98})$	*f* = 13.75	*f* = 1.60	*f* = 9.38

Table 7. The percentages of individual crystal phases (f/%), obtained using the software package Powder Cell, of examined samples in the fraction −10 + 0 μm.

Phase	JKB −10 + 0 μm	JOF −10 + 0 μm	JPH −10 + 0 μm
Quarz; SiO_2	f = 7.51	f = 6.84	f = 7.35
Pyrite; FeS_2 *Cubic*	f = 1.30	f = 1.13	f = 0.42
Clinochlore; $Mg_{2.5}Fe_{1.65}Al_{1.5}Si_{2.2}Al_{1.8}O_{10}(OH)_8$	f = 37.65	f = 42.09	f = 47.59
Calcite; $CaCO_3$	f = 9.45	f = 14.17	f = 10.87
Albite; Na ($AlSi_3O_8$)	f = 40.13	f = 27.44	f = 33.47
Biotite; $K_2(Mg_{3.15}Fe_{2.59}Ti_{0.17}Mn_{0.09})(Si_{5.98}Al_{1.92}Ti_{0.10})O_{20}$ $((OH)_{1.47}F_{1.98})$	f = 3.96	f = 8.33	f = 0.30

In Figure 4 and Tables 4 and S2 are given the results of the XRD analyses of the mineral composition and parameters of the unit cell of the sample JKB after separation into fractions. From the presented results, it is evident that mineral composition has been significantly changed after separation. In addition, every fraction significantly differs in mineral composition in comparison with the others. It is important to note that the contents of the minerals that may have a potential application (albite, calcite and biotite) change significantly depending on which fraction is involved. The highest percentage of calcite (~52%) was in the fraction −63 + 0 μm, which is four times higher in comparison with the starting JKB sample. The content of the albite was about 4.5 times lower in this fraction, while the biotite content remained almost unchanged. The total amount of the minerals which do not possess significant useful values (clinochlore (~22%), quartz (~5%) and pyrite (~8%)) was about 36%. The highest content of the albite (~68%) was obtained in the fraction −300 + 200 μm. For this fraction, the contents of biotite and calcite were very low (<2%). The content of quartz was ~27%, and clinochlore ~3%. In this fraction, pyrite was not detected. The content of biotite was the highest in the fraction −400 + 300 μm. However, this fraction contained a significant amount of quartz (~36%) and clinochlore (~26%). The content of pyrite was very low (0.03%). This fraction contained albite ~20% and calcite about 5%. In other fractions in the range −200 + 63 μm, the largest amount of quartz was detected (averaged ~35%). The average amount of albite was ~ 27%, calcite about 11%, and biotite about 9.5%. Considering that the results presented in Table 4 show that the most prevalent are fractions −200 + 100, −100 + 63 and −63 + 0 μm (in total 95.53%), it can be concluded that the extraction of useful minerals will be cost-effective only from these three fractions.

For the JOF sample, the following fractions were analyzed: −63 + 0 μm, −100 + 63 μm, −200 + 100 μm, −300 + 200 μm, −400 + 300 μm and +400 μm, and results are given in Figure 5 and Tables 5 and S3.

From Figure 5, it is evident that after fractionization of the JOF sample, the content of detected mineral phases significantly changed. The composition of individual fractions differs from the others. From Figure 5b, it is clear that the content of calcite increases for lower particle size in comparison with the starting JOF sample. For the fractions −63 + 0 μm and −100 + 63 μm, the calcite content was ~22%, and maximal calcite content was obtained in the fraction −200 + 100 μm (~52%). In other fractions (+200 μm), the content of the calcite was much lower, in the range ~1–6%. The content of albite in all fractions in the range −400 + 0 μm was lower in comparison with the starting sample (Figure 2b, 28.15%) and only in fraction +400 μm was a significantly higher amount of this mineral detected (~45%). The samples with a particle size of −300 + 0 μm contained smaller amounts of biotite than the starting sample (maximal 7.71%). In fractions with a particle size of +200 μm, significantly larger quantities of this mineral were detected (~12% for the fraction −400 + 300 μm and ~15% for the fraction +400 μm). The quartz content varied in the range of 10–50%, while that of pyrite to a maximum of 5%, and the clinochlore content

varied in the range of 13 to 42%. Considering the results presented in Table 5, the most prevalent are fractions −300 + 200, −200 + 100, −100 + 63 and −63 + 0 μm (in total 92%), and the extraction of useful minerals will be cost-effective only from these three fractions.

For the JHC sample, fractions 63 + 0, −100 + 63 and −200 + 100 μm were analyzed. As can be seen from the results presented in Table 6, there are no particles in the particle size range +400, −400 + 300 and −300 + 200 μm. The XRD diffractograms are given in Figure 6, while the percentage compositions of fractions and crystal parameters are given in Figure 6 and Tables 6 and S4. From the obtained results, it can be concluded that the compositions of the different fractions is not uniform and there is a difference in the mineral contents. Also, the composition differs significantly from the starting JHC sample. The highest (~24%) and the lowest (~13%) amounts of albite were determined in fractions −200 + 100 and −100 + 63 μm, respectively. The highest amount of biotite (~14%) was in the fraction −100 + 63 μm, while highest amount of calcite was in the fraction −63 + 0 and −100 + 63 μm. Auxiliary minerals such as quartz and clinochlore were mostly present (more than 50%) in this sample regardless of the particle size and fraction. Considering that, the results presented in Table 6 show that the most prevalent is fraction −63 + 0 μm (91.33%), and it can be concluded that the extraction of useful minerals will be cost-effective from this fraction.

In general, materials with the smallest particle size are the most problematic for their potential application in various technological processes. The fraction −63 + 0 μm is significantly present in all three samples (91.33% for JHC, 33.27% for JOF and 16.73% for JKB). For that reason, it was of interest to determine the composition of fractions with the finest degree of granulation. For that purpose, the JKB, JOF and JHC samples were additionally sieved and the mineralogical composition of the fraction with a particle size of −10 + 0 μm was examined. The contribution of this fraction was not negligible for JOF (10.11%) and JHC (15%), while for JKB, it was only 3.2%. However, to compare results, all three samples were analyzed with XRD and the results are presented in Figure 7 and Tables 7 and S5.

It may be noted from Figure 7 that for all three samples, the changes in phase composition are not uniform in comparison with the starting samples (Figure 2b). All phases in the starting JKB, JOF and JPH samples were detected in this fraction, but in a different relation. For the JKB sample, in the fraction −10 + 0 μm, the contents of the quartz (~8%), calcite (~10%) and pyrite (~1%) were lower, while the content of the biotite (~4%), clinochlore (~38%) and albite (~40%) were higher in comparison with the starting sample. For the JOF sample, the content of the albite, calcite, biotite and pyrite was approximately equal to the content in the starting sample, while the content of quartz (~7%) was lower and clinochlore (~42%) was higher. For the JHC sample, in the fraction −10 + 0 μm, only the content of the albite (~48%) increased, and the content of quartz (~7%) decreased, while the content of other mineral phases was approximately equal as in the starting JHC sample. From the presented results, considering the presence of this fraction (Table 3), it can be concluded that the extraction of useful minerals will be cost-effective from this fraction only in JHC and JOF.

After the identification of fractions in which the contents of useful minerals are the highest, it is possible to further extract them by using appropriate techniques. For example, albite and biotite may be extracted and separated from useless minerals by using gravity and magnetic separation techniques [27], and calcite by using flotation technique and anionic/cationic collectors [28].

Regarding the application of useful minerals, they are used in various industrial processes. *Calcite* can be used in non-ferrous metals and minerals, iron and steel, chemicals, portable water, pulp and paper, oil & gas, cement and construction, agriculture, animal husbandry and aquaculture, as well as in wastewater and sludge treatment, sugar refining, flue gas treatment, glass and ceramics, road and soil stabilization, food preparation, supplements and many more. Specifically in the construction industry, calcite plays an important role in concrete. It can not only reduce the cost of production but also increase the

toughness and strength of the product (for example, requirements for dry mortar: particle size, 325; mesh whiteness, 95%; $CaCO_3$ content, 98%). Likewise, in the paper-making industry, if the whiteness of calcium carbonate is above 90%, it can replace the expensive white pigment and calcite as a paper filler, it can guarantee the strength and whiteness of the paper, and therefore less wood will be used, and the cost will be lower [29].

When it comes to *albite*, its use and demand might vary over time based on availability and market trends. These are some of its key applications: Ceramics: as a raw material, particularly in the production of porcelain, tiles, and other ceramic products, for example. Requirements for albite: the content of K_2O and Na_2O should be as high as possible, and the content of the colored oxides Fe_2O_3 and TiO_2 should be as low as possible; the content of SiO_2 should be in the range of 63–68%, and the content of Ali_2O_3 should be in the range of 17–23%). It helps improve the strength and durability of the ceramics; Glass manufacturing: Albite is used as a fluxing agent, which reduces the melting temperature of the glass and helps to control its viscosity during the production process; Construction materials: Albite can be used as an aggregate in concrete and asphalt. It contributes to the strength and stability of these materials; Fillers and extenders: Albite is used as a filler or extender in various products, such as paints, coatings, plastics, and rubber. It helps to improve the mechanical properties of these materials and reduce production costs; Refractory materials: Albite is utilized in the manufacturing of refractory materials, which are heat-resistant materials used in high-temperature applications like furnaces and kilns [30].

Biotite, although less common than muscovite, can be used as a filler material in various industrial products. It can be added to paints, plastics, and other materials to improve their properties because it has good slip, luster and shine properties. Due to its great thermal and electrical insulating properties, biotite in the form of thin sheets (its hardness on the Mohs scale has a value between 2, 5 and 3 and its density is 3.09) can be used as an insulating material in some specialized applications, such as part of the walls and windows of microwave ovens or in the field of electronics for manufacturing capacitors and transistors. In addition, it is important to note that biotite plays an important role in radiometric dating techniques such as potassium–argon dating to determine the age of rocks and geological events. This is especially important for geological and mineralogical studies [31].

It is important to point out that this paper presents laboratory research. The available literature on recovery methods in semi-industrial and industrial plants is very limited. All knowledge about recovery methods is based on laboratory research, so developing technologies for obtaining useful elements and minerals from mine waste is a new field of exploitation and recovery. In addition, there is still no universal legal regulation that could be applied at the global level which refers to the exploitation of such deposits. The recovery of useful elements from mine tailings is being tested all over the world; however, the composition of mine waste and the methods of preparation and processing of mineral raw materials vary significantly from mine to mine. For this reason, it is still not possible to perform a techno-economic evaluation of the process. It is expected that, in the field of economics and profitability of this type of mining, a larger number of studies will be conducted in the future.

4. Conclusions

The Grot Mine tailings pond is a flotation dump in the Republic of Serbia. The geochemical characteristics of the tailings pond depend on the composition of the exploited ore bodies, concentrations of metals at the inlet of flotation, and yields in the flotation process. This work aimed to determine whether these waste materials can be reused and applied for different purposes in terms of their mineralogical and morphological characterization. After a detailed structural, morphological and geochemical analysis of samples taken from three different tailings sites (JKB, JOF and JHC), the results showed that the mineral content significantly depends on which tailings fraction is examined. The highest (~24%) and the lowest (~13%) amounts of albite were determined in the fractions

−200 + 100 and −100 + 63 μm, respectively. The highest amount of biotite (~14%) was in the fraction −100 + 63 μm, while the highest amount of calcite was in the fraction −63 + 0 and −100 + 63 μm. Auxiliary minerals such as quartz and clinochlore were mostly present (more than 50%) in this sample regardless of the particle size and fraction. Results show that the most prevalent was the fraction −63 + 0 μm (91.33%); therefore, these fractions are the most important to examine and recover for further use. Namely, considering that all samples consisted mostly of silicate and alumosilicate minerals of micro and nano size, it can be said that the examined waste materials have great potential to be used as a secondary mineral raw material source, applicable in various industries such as the construction, electronic, agricultural or energy sectors, for the production of fine-sized ceramics, glass, refractory products, abrasives, adhesives, coatings, etc., specifically in the manufacturing of glass or ceramic (albite), in the lime production and construction industry (calcite), and as a filler and extender in paints, an additive to drilling muds, and an inert filler and mold-release agent in rubber products (biotite).

However, further research is required to determine the ecological safety and proper efficiency of these materials, depending on particular applications. In the first place, the presence and leaching of heavy metals and the physical-mechanical features need to be evaluated, and their performance in operating conditions should be demonstrated as well. The major objective of this study is aimed towards obtaining efficient and cost-effective materials from waste products for natural resource conservation as well as environmental protection by minimizing the negative effects of primary production.

Supplementary Materials: The following supporting information can be downloaded at: https://www.mdpi.com/article/10.3390/app14031167/s1.

Author Contributions: Conceptualization, J.G., M.K. and M.S.; methodology, J.G., M.K. and M.S.; validation, J.G., M.K. and M.S.; formal analysis, J.G.; investigation, A.V., I.R., M.R. and I.J.-Č.; writing—original draft preparation, J.G., M.K. and M.S.; writing—review and editing, J.G.; supervision, J.G., M.K. and M.S. All authors have read and agreed to the published version of the manuscript.

Funding: This research received no external funding.

Institutional Review Board Statement: Not applicable.

Informed Consent Statement: Not applicable.

Data Availability Statement: The data presented in this study are available on request from the corresponding author. The data are not publicly available due to privacy.

Acknowledgments: Results published in this paper are a part of the investigations supported by the Ministry of Science, Technological Development and Innovation of the Republic of Serbia (Contract numbers 451-03-47/2023-01/200017) through the realization of research themes 1702303, 1702305 and 1702314. This research was also supported by an Eit Raw Materials project 21043 Reco2Mag—"Grain boundaries engineered Nd-Fe-B permanent magnets".

Conflicts of Interest: The authors declare no conflicts of interest.

References

1. Kamberović, Z.; Radović, N.; Korać, M.; Jovanović, M. The strategy for cleaner production in the Metallurgy of Republic of Serbia. In *Proceedings, II Symposium "Recycling Technologies and Sustainable Development" with International Participation*; Faculty of Engineering in Bor, University of Belgrade, Department of Mineral and Recycling Technologies: Sokobanja, Serbia, 2007; pp. 284–291.
2. Đokić, B.V. The need to establish sincere relationships between nature and man. In *Proceedings, II Symposium "Recycling Technologies and Sustainable Development" with International Participation*; Faculty of Engineering in Bor, University of Belgrade, Department of Mineral and Recycling Technologies: Sokobanja, Serbia, 2003; pp. 68–75.
3. Janković, S.; Jelenković, R.; Vujić, S. *Mineral Resources and Potential Prediction of Metallic and Non-Metallic Mineral Resources of Serbia and Montenegro at the End of the 20th Century*; Engineering Academy of Serbia and Montenegro: Belgrade, Serbia, 2003.
4. Janković, S. Mining deposits of Serbia. In *Regional Metallogenetic Position, Midpoints, and Bearing Types. Republican Social Fund for Geological Research*; University of Belgrade, Faculty of Mining and Geology: Belgrade, Serbia, 1990.

5. Milićević, V.; Starčević, M.; Simić, M.; Milanković, M. *Metallogeny of the Mačkatica-Blagodat-Karamanica Zone*; Geoinstitute Special Editions: Belgrade, Serbia, 2001.
6. Đokić, B.V. *Geochemical Characteristics of the Grot Mine Flotation Site (Southeastern Serbia)*; University of Belgrade, Faculty of Mining and Geology: Belgrade, Serbia, 2012.
7. Ranđelović, D.; Mutić, J.; Marjanović, P.; Đorđević, T.; Kašanin-Grubin, M. Geochemical distribution of selected elements in flotation tailings and soils/sediments from the dam spill at the abandoned antimony mine Stolice, Serbia. *Environ. Sci. Pollut. Res.* **2020**, *27*, 6253–6268. [CrossRef] [PubMed]
8. Araya, N.; Kraslawski, A.; Cisternas, L.A. Towards mine tailings valorization: Recovery of critical materials from Chilean mine tailings. *J. Clean. Prod.* **2020**, *263*, 121555. [CrossRef]
9. El Wali, M.; Golroudbary, S.R.; Kraslawski, A. Impact of recycling improvement on the life cycle of phosphorus. *Chin. J. Chem. Eng.* **2019**, *27*, 1219–1229. [CrossRef]
10. United Nations Sustainable Development Goals (SDGs). Available online: https://www.un.org/sustainabledevelopment/sustainable-development-goals/? (accessed on 18 December 2023).
11. Šajn, R.; Ristović, I.; Čeplak, B. Mining and Metallurgical Waste as Potential Secondary Sources of Metals—A Case Study for the West Balkan Region. *Minerals* **2022**, *12*, 547. [CrossRef]
12. Stojmenović, M.; Pašalić, S.; Kragović, M. Influence of the underground mining waste on the environmental tailings and wastewater characterization. *Undergr. Min. Eng.* **2017**, *31*, 85–100. [CrossRef]
13. Kraus, W.; Nolze, G. POWDER CELL–a program for the representation and manipulation of crystal structures and calculation of the resulting X-ray powder patterns. *J. Appl. Crystallogr.* **1996**, *29*, 301–303. [CrossRef]
14. PowderCell for Windows 2.4, Software. Available online: http://powdercell-for-windows.software.informer.com/2.4/ (accessed on 15 February 2019).
15. American Mineralogist Crystal Data Structure Base (AMCDSB). (n.d.) Software. Available online: http://rruff.geo.arizona.edu/AMS/amcsd.phpS (accessed on 15 November 2023).
16. Voinovitch, I.; Debrad-Guedon, J.; Louvrier, J. *The Analysis of Silicates*; Israel Program for Scientific Translations: Jerusalem, Israel, 1966.
17. Bo, F.; Xianping, L.; Jinqing, W.; Pengcheng, W. The flotation separation of scheelite from calcite using acidified sodium silicate as depressant. *Miner. Eng.* **2015**, *80*, 45. [CrossRef]
18. Tao, H.; Dongwei, L. Presentation on mechanisms and applications of chalcopyrite and pyrite bioleaching in biohydrometallurgy—A presentation. *Biotechnol. Rep.* **2014**, *4*, 107–119. [CrossRef] [PubMed]
19. Karagüzel, C. Selective separation of fine albite from feldspathic slime containing colored minerals (Fe-Min) by batch scale dissolved air flotation (DAF). *Miner. Eng.* **2010**, *23*, 17–24. [CrossRef]
20. Zhang, W.Y.; Gao, H.; Xu, Y. Sintering and reactive crystal growth of diopsidealbite glass–ceramics from waste glass. *J. Eur. Ceram.* **2011**, *31*, 1669–1675. [CrossRef]
21. Wang, J.; Gao, Z.; Gao, Y.; Hu, Y.; Sun, W. Flotation separation of scheelite from calcite using mixed cationic/anionic collectors. *Miner. Eng.* **2016**, *98*, 261–263. [CrossRef]
22. Xing, P.; Wang, C.; Ma, B.; Wang, L.; Zhang, W.; Chen, Y. Rubidium and potassium extraction from granitic rubidium ore: Process optimization and mechanism study. *ACS Sustain. Chem. Eng.* **2018**, *6*, 4922–4930. [CrossRef]
23. Wang, W.; Sun, J.; Dong, C.; Lian, B. Biotite weathering by Aspergillus niger and its potential utilization. *J. Soils Sediments* **2016**, *16*, 1901–1910. [CrossRef]
24. Małgorzata Labus, Pyrite thermal decomposition in source rocks. *Fuel* **2021**, *287*, 119529. [CrossRef]
25. Mackenzie, R.C. *Differential Thermal Analysis*; Academic Press INC: New York, NY, USA; London, UK, 1970.
26. Steudel, A.; Kleeberg, R.; Koch, C.B.; Friedrich, F.; Emmerich, K. Thermal behavior of chlorites of the clinochlore-chamosite solid solution series: Oxidation of structural iron, hydrogen release and dehydroxylation. *Appl. Clay Sci.* **2016**, *132*, 626–634. [CrossRef]
27. El-Sayed, H.R.E.; Abdel-Khalek, N.A.; Youssef, M.A.; Abdallah, M.M.; El-Menshawy, A.H. Recovery of Albite and Mica from Egyptian Abu Dabbab Ores Using Gravity and Magnetic Separation Techniques. *AJBAS* **2017**, *11*, 115–123.
28. Drzymala, J. *Mineral Processing: Foundations of Theory and Practice of Metallurgy*; University of Technology: Wroclaw, Poland, 2007.
29. Available online: https://mill.zenith-mills.com/products/?a= (accessed on 23 January 2024).
30. Available online: https://www.lsalloy.com/?s=albite&search_form_submit= (accessed on 23 January 2024).
31. Available online: https://geologyscience.com/minerals/biotite/?amp (accessed on 23 January 2024).

Disclaimer/Publisher's Note: The statements, opinions and data contained in all publications are solely those of the individual author(s) and contributor(s) and not of MDPI and/or the editor(s). MDPI and/or the editor(s) disclaim responsibility for any injury to people or property resulting from any ideas, methods, instructions or products referred to in the content.